Chemical Research in Toxicology

Article

pubs.acs.org/crt

Highly Predictive Reprogramming of tRNA Modifications Is Linked to Selective Expression of Codon-Biased Genes

Clement T. Y. Chan,[†,⊥,▽] Wenjun Deng,[†,#,▽] Fugen Li,[‡,○] Michael S. DeMott,[†] I. Ramesh Babu,[†] Thomas J. Begley,[∥] and Peter C. Dedon*[,†,§]

[†]Department of Biological Engineering, [‡]BioMicro Center, [§]Center for Environmental Health Sciences, Massachusetts Institute of Technology, Cambridge, Massachusetts 02139, United States

[∥]College of Nanoscale Science, State University of New York, Albany, New York 12203, United States

Supporting Information

ABSTRACT: Cells respond to stress by controlling gene expression at several levels, with little known about the role of translation. Here, we demonstrate a coordinated translational stress response system involving stress-specific reprogramming of tRNA wobble modifications that leads to selective translation of codon-biased mRNAs representing different classes of critical response proteins. In budding yeast exposed to four oxidants and five alkylating agents, tRNA modification patterns accurately distinguished among chemically similar stressors, with 14 modified ribonucleosides forming the basis for a data-driven model that predicts toxicant chemistry with >80% sensitivity and specificity. tRNA modification subpatterns also distinguish S_N1 from S_N2 alkylating agents, with S_N2-induced increases in m^3C in tRNA mechanistically linked to selective translation of threonine-rich membrane proteins from genes enriched with ACC and ACT degenerate codons for threonine. These results establish tRNA modifications as predictive biomarkers of exposure and illustrate a novel regulatory mechanism for translational control of cell stress response.

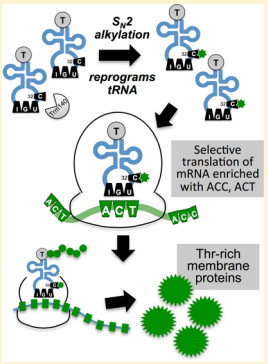

INTRODUCTION

Cells respond to environmental stressors and xenobiotic exposures by controlling gene expression with multilayered, complex regulatory networks. The emergence of tools to quantify the molecular changes associated with these networks has led to an appreciation for the mechanistic insights and predictive power derived from transcriptional profiling, proteomics, and metabolomics.[1−5] Using a novel bioanalytical platform, we recently described an example of another network that regulates the cellular response to xenobiotic exposures and other stresses: stress-induced reprogramming of a system of two-dozen post-transcriptional modifications on tRNA (tRNA), which promotes selective translation of codon-biased mRNAs for critical response proteins.[6−8] Most forms of RNA contain modified ribonucleosides, with more than 120 different chemical structures across all organisms and 2−3 dozen in any one organism.[9,10] tRNA is the most extensively modified RNA species, with the presence of specific ribonucleoside structures affecting the rate and fidelity of translation,[11,12] tRNA stability,[13,14] cellular stress responses,[6,15,16] and cell growth.[17] To define a systems-level behavior for tRNA modifications, we developed a chromatography-coupled tandem quadrupole mass spectrometry (LC-MS/MS) method to quantify stress-induced changes in the system of modified ribonucleosides in a population of cellular tRNA molecules or in individual, purified tRNA species.[7,8,18−20] We applied this approach to budding yeast exposed to four mechanistically different toxicants (hydrogen peroxide, H_2O_2; methylmethanesulfonate, MMS; sodium arsenite $NaAsO_3$; and sodium hypochlorite, NaOCl) and observed agent-specific changes in the relative quantities of 23 modified ribonucleosides in tRNA.[7] These results pointed to the spectrum of modified ribonucleosides in tRNA as a predictive biomarker of exposure. Furthermore, stress-specific reprogramming of tRNA wobble modifications was found to result in selective translation of mRNAs containing biased use of the codons corresponding to these tRNAs, with the mRNAs representing critical stress response proteins.[6−8]

These observations were made with four chemically distinct toxicants, which raised questions about the specificity of the tRNA reprogramming signatures for classes of chemical toxicants (e.g., all oxidants) and the generality of the translational response mechanism. To test the hypothesis that cells respond to mechanistically similar toxicants with similar patterns of tRNA modification reprogramming and that the patterns are predictive of the chemical class of the toxicant, we analyzed changes in the levels of 23 modified ribonucleosides in tRNA from *Saccharomyces cerevisiae* exposed to four oxidizing agents (hydrogen peroxide (H_2O_2), *t*-butyl hydroperoxide (TBHP), γ-radiation (γ-rad), and peroxynitrite ($ONOO^-$)) and five alkylating agents (methylmethanesulfonate (MMS), ethylmethanesulfonate (EMS), isopropyl methanesulfonate (IMS), *N*-methyl-*N*′-nitro-*N*-nitrosoguanidine (MNNG), and *N*-nitro-*N*-methylurea (NMU)). Multivariate statistical analysis and data-driven modeling of the RNA modification patterns

Received: January 3, 2015
Published: March 14, 2015

DOI: 10.1021/acs.chemrestox.5b00004
Chem. Res. Toxicol. 2015, 28, 978−988

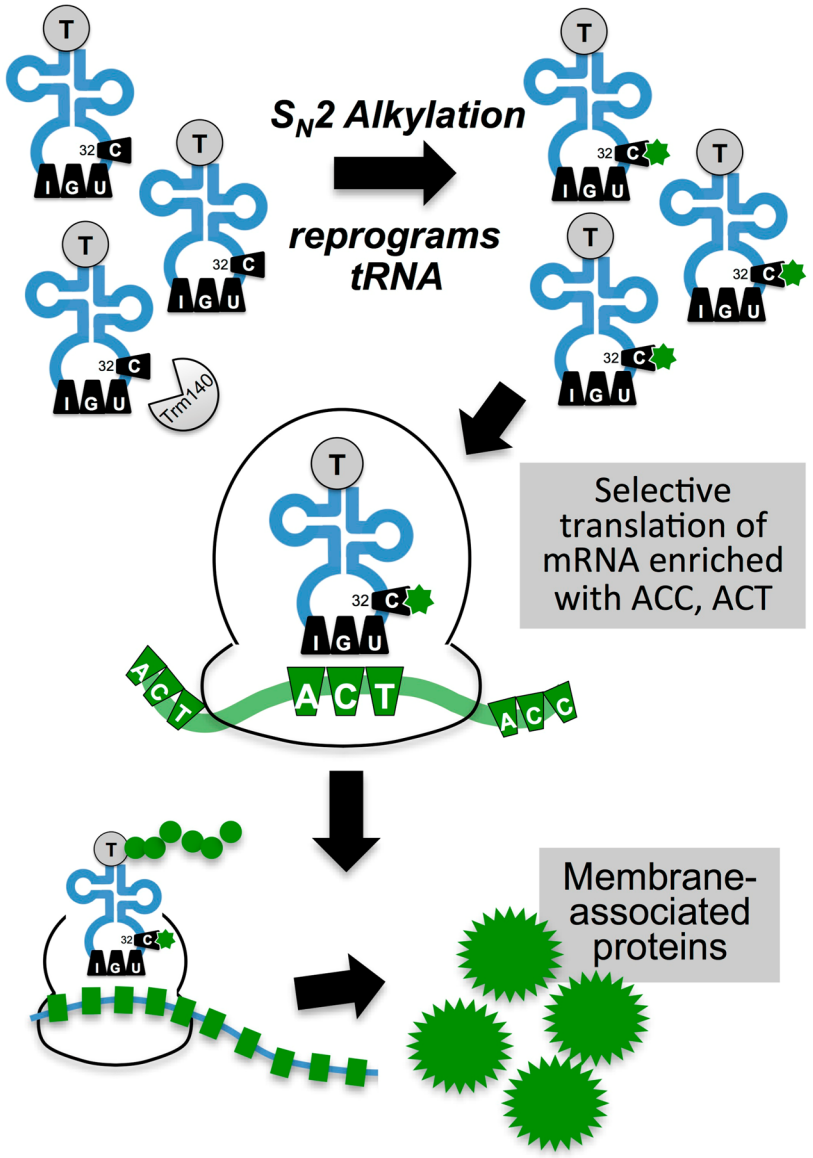

Figure 1. Proposed model for stress-specific reprogramming of tRNA modifications leading to selective translation of codon-biased response proteins. The specific model shown here is based on exposure to the S_N2 alkylating agent, methylmethanesulfonate (MMS), which leads to upregulation of the modified ribonucleoside m^3C in tRNA species coding for threonine and serine, with their cognate codons enriched (ACC, ACT) in membrane-associated proteins. This model is consistent with broad mechanisms for MMS-induced toxicity proposed by Smith and Grisham.[50]

proved to be highly predictive of toxicant chemistry, with bioinformatic and proteomic analyses establishing a mechanistic link among exposure, tRNA modifications, and codon-biased translation of response proteins. The results support a 30 year old model for one of the mechanisms by which S_N2 alkylating agents promote cell death, by damaging membrane proteins, and establish a novel regulatory mechanism linking exposure to translational response in cells, which is summarized in Figure 1.

EXPERIMENTAL PROCEDURES

Materials. All chemicals and reagents were of the highest purity available and were used without further purification. MMS, EMS, NMU, TBHP, H_2O_2, RNase A, and alkaline phosphatase were obtained from Sigma Chemical Co. (St. Louis, MO). IMS was obtained from Pfaltz & Bauer, Inc. (Waterbury, CT). MNNG was obtained from TCI America (Portland, OR). Sodium peroxynitrite was obtained from Cayman Chemical Co. (Ann Arbor, MI). Nuclease P1 was obtained from Roche Diagnostic Corp. (Indianapolis, IN). Phosphodiesterase I was obtained from USB (Cleveland, OH). Yeast extract and peptone were obtained from Biomed Diagnostics, Inc. (White City, OR). Micron YM10 filters were obtained from PALL Corp. (Port Washington, NY). HPLC-grade water and acetonitrile were obtained from Mallinckrodt Baker (Phillipsburg, NJ). *S. cerevisiae* BY4741 was obtained from American Type Culture Collections (Manassas, VA).

***S. cerevisiae* Cytotoxicity Dose–Response Assays.** *S. cerevisiae* BY4741 was cultured in YPD (yeast extract-peptone-dextrose) media with 200 μg/mL of geneticine at 30 °C with shaking at 220 rpm. Each culture was grown to mid log phase (OD_{660} ~ 0.6–0.8) followed by exposure to the following toxicants and concentrations: H_2O_2 (0, 2, 3.5, 5, 10, 15, and 20 mM), TBHP (0, 0.7, 2, 4, 7, 14, 22, 25, and 29 mM), $ONOO^-$ (0, 0.3, 0.5, 0.8, 1.0, 1.5, and 2.0 mM), γ-rad (116 Gy/min) (0, 21.3, 168, 327, 513, and 606 Gy), MMS (0, 1.2, 6, 12, 24, 36, and 48 mM), EMS (0, 0.19, 0.29, 0.39, 0.49, and 0.58 M), IMS (0, 8, 17, 33, 50, and 66 mM), MNNG (0, 41, 61, 82, 102, and 136 mM), and NMU (0, 1.3, 2.3, 3.2, and 4.2 mM). After 1 h at 30 °C, these cultures were diluted 10^4-fold with YPD medium, and 50 μL was plated on YPD agar. Survival rates of exposed cells were determined by

DOI: 10.1021/acs.chemrestox.5b00004
Chem. Res. Toxicol. 2015, 28, 978–988

comparing colony counts for untreated and treated samples after 2 days of growth.

Cell Exposure and tRNA Isolation. Cultures of *S. cerevisiae* at mid log phase (OD_{660} ~ 0.6; ~2 × 10^7 cells) were treated with 5 mM H_2O_2, 25 mM TBHP, 0.8 mM $ONOO^-$, 500 Gy γ-rad (116 Gy/min), 24 mM MMS, 190 mM EMS, 50 mM IMS, 82 mM MNNG, or 3.2 mM NMU and incubated for 1 h at 30 °C alongside untreated control cultures. Cells were pelleted by centrifugation and resuspended in TRIzol reagent with the addition of antioxidants (0.1 mM desferrioxamine and 0.1 mM butylated hydroxytoluene) and deaminase inhibitors (5 μg/mL coformycin and 50 μg/mL tetrahydrouridine). Cells in this solution were lysed by three cycles of bead beating in a Thermo FP120 bead beater at 6.5 m/s for 20 s each cycle, with 1 min of cooling on ice between cycles. The lysates was mixed with one-volume of chloroform, and phases were separated by centrifugation. Small RNA in the aqueous phase was isolated using using the PureLink miRNA isolation kit according to manufacturer's instructions. Each sample yielded ~6 μg of RNA composed of ~90% tRNA, as judged by Bioanalyzer analysis (Agilent Corporation).

Quantification of tRNA Modifications. tRNA modifications were quantified using an established LC-MS/MS method,[7] which starts with hydrolysis of tRNA (6 μg) in a solution (50 μL; pH 6.8) containing 30 mM sodium acetate, 2 mM $ZnCl_2$, 0.02 unit/μL of nuclease P1, 0.1 unit/μL of RNase A, 5 μg/mL coformycin, 50 μg/mL tetrahydrouridine, 0.1 mM deferoxamine mesylate, 0.1 mM butylated hydroxytoluene, and 6 pmol of $[^{15}N]_5$-2′-deoxyadenosine ($[^{15}N]_5$-dA) as an internal standard. Following incubation at 37 °C for 3 h, the solution was augmented (additional 50 μL volume) with an additional 30 mM sodium acetate, 0.2 unit/μL of alkaline phosphatase, and 0.01 unit/μL of phosphodiesterase I at a final pH of 7.8 and incubated 37 °C overnight. Proteins were removed by centrifugal ultrafiltration using a Microcon YM-10 filter. An aliquot of filtrate containing ~0.4 μg of ribonucleosides was loaded on a Thermo Scientific Hypersil GOLD aQ reverse-phase HPLC column (150 × 2.1 mm, 3 μm particle size), and ribonucleosides were eluted with the following gradient of acetonitrile in 8 mM ammonium acetate at a flow rate of 0.3 mL/min at 36 °C: 0–18 min, 0%; 18–23 min, 0–1%; 23–28 min, 1–6%; 28–30 min, 6%; 30–40 min, 6–100%; 40–50 min, 100%. The HPLC column was coupled to an Agilent 6410 Triple Quadrupole LC/MS mass spectrometer with an electrospray ionization source operated in positive ion mode with the following parameters: gas temperature, 350 °C; gas flow, 10 L/min; nebulizer, 20 psi; and capillary voltage, 3500 V. The first and third quadrupoles (Q1, Q3) were fixed to unit resolution, and the modifications were quantified by predetermined molecular transitions. Q1 was set to transmit the parent ribonucleoside ions, and Q3 was set to monitor the deglycosylated product ions, except for pseudouridine (Y), which was detected by setting Q1 to transmit the parent ion and Q3 set to monitor the m/z = 125 product ion resulting from pyrimidine ring fragmentation.[7,21] The dwell time for each ribonucleoside was 200 ms. The retention time, m/z of the transmitted parent ion, m/z of the monitored product ion, fragmentor voltage, and collision energy of each modified nucleoside and ^{15}N-labeled internal standard are as follows: D, 2.2 min, m/z 247 → 115, 80 V, 5 V; Y, 2.3 min, m/z 245 → 125, 80 V, 10 V; m^5C, 5.4 min, m/z 258 → 126, 80 V, 8 V; Cm, 6.4 min, m/z 258 → 112, 80 V, 8 V; m^5U, 7.9 min, m/z 259 → 127, 90 V, 7 V; ncm^5U, 8.7 min, m/z 302 → 170, 90 V, 7 V; ac^4C, 19.0 min, m/z 286 → 154, 80 V, 6 V; m^3C, 5.0 min, m/z 258 → 126, 80 V, 8 V; Um, 10.7 min, m/z 259 → 113, 90 V, 7 V; m^7G, 8.5 min, m/z 298 → 166, 90 V, 10 V; m^1A, 6.9 min, m/z 282 → 150, 100 V, 16 V; mcm^5U, 14.6 min, m/z 317 → 185, 90 V, 7 V; m^1I, 16.0 min, m/z 283 → 151, 80 V, 10 V; Gm, 17.2 min, m/z 298 → 152, 80 V, 7 V; m^1G, 18.8 min, m/z 298 → 166, 90 V, 10 V; m^2G, 22.2 min, m/z 298 → 166, 90 V, 10 V; I, 7.8 min, m/z 269 → 137, 80 V, 10 V; mcm^5s^2U, 31.3 min, m/z 333 → 201, 90 V, 7 V; $[^{15}N]_5$-dA, 30.0 min, m/z 257 → 141, 90 V, 10 V; $m^2{}_2G$, 31.7 min, m/z 312 → 180, 100 V, 8 V; t^6A, 32.8 min, m/z 413 → 281, 100 V, 8 V; Am, 33.1 min, m/z 282 → 136, 100 V, 15 V; yW, 34.1 min, m/z 509 → 377, 120 V, 10 V, and i^6A, 34.5 min, m/z 336 → 204, 120 V, 17 V. The signal from each modified nucleoside was normalized by dividing by the signal from $[^{15}N]_5$-dA for the purpose of comparison between samples. Complete analysis was performed as technical duplicates of each of five biological replicates, with samples from each biological replicate analyzed as a single batch to minimize the influence of day-to-day variation in instrument performance.

Data Analysis. Exposure-induced changes in the quantities of modified ribonucleosides were calculated as fold-change values using the normalized MS signal intensities for the treated and unexposed samples. This was accomplished by averaging the normalized MS signal intensity for each ribonucleoside in the three control samples and then dividing the corresponding normalized MS signal intensity for each ribonucleoside in each treated sample by this average control value. These fold-change values are presented in Table S1, and the mean (±standard deviation) fold-change values for the five replicates are presented in Table S2. The fold-change values were then analyzed by hierarchical clustering using the centroid linkage algorithm in Cluster 3.0 following $\log_2$ transformation of the fold-change data; heat map representations were produced using Java Treeview, as described elsewhere.[7] The heat map for the entire data set is shown in Figure S3, and that for the averaged data, in Figure 3.

Data-Driven Modeling. To assess the predictive power of the stress-altered tRNA modification patterns, the normalized MS signal intensities for each biological replicate of treated and control cells was used to develop a data-driven model (Figure 4A). The data for individual samples were labeled as one of three classes of toxicant exposure: unexposed control (CT), alkylating agent-exposed (AA), and oxidizing agent-exposed (OX). A classification model was then developed using K-nearest neighbor classification. From each exposure class, normalized ribonucleoside signal intensities were compared to the other classes using multiple *t*-tests with Bonferroni correction, and those with p values < 0.01 were assigned as unique features of that exposure group. All of these unique features were then set as parameters to construct a data-driven model using the programming software R, in which all data were randomly assigned into two groups: a training set to build the model and a testing set to evaluate the prediction accuracy of the model. For this evaluation, the confusion matrix method (Figure 4B) was used to determine prediction sensitivity and prediction specificity.

SILAC Proteomics. MMS-induced changes in protein levels were determined by SILAC proteomics.[8,22] To prepare isotopically labeled proteins, *Lys1*Δ yeast cells were grown in yeast nitrogen base (YNB) liquid medium containing 30 mg/L of L-lysine-U-$[^{13}C]_6$, $[^{15}N]_2$ (Isotec-SIGMA, Miamisburg, OH) for at least 10 generations, until they reached log-phase (OD_{600} ~ 0.7).[23] Wild-type yeast cells were grown to log phase (OD_{600} ~ 0.7) in YNB medium containing 30 mg/L of L-lysine. Cells were harvested by centrifugation at 1500*g* for 10 min at 4 °C and washed twice with ice-cold water. Cells were then lysed by suspension in alkaline buffer (2 M NaOH, 8% 2-mercaptoethanol v/v), and proteins were precipitated by adding 50% TCA and incubating on ice for 10 min, followed by centrifugation at 15 000*g* for 15 min at 4 °C. The pellet was resuspended in lysis buffer (8 M urea, 75 mM NaCl, 50 mM Tris, pH 8.2, 50 mM NaF, 50 mM β-glycerophosphate, 1 mM sodium orthovanadate, 10 mM sodium pyrophosphate, 1 mM phenylmethylsulfonyl fluoride).[24] Protein concentration was determined by the Bradford assay.[25] Heavy SILAC-labeled *lys1*Δ yeast proteins were used as a global internal standard.[26] For the MMS exposure studies, cells (OD_{600} ~ 0.7) were treated for 1 h with 0.0125% MMS in YNB media at 30 °C, which caused less than 5% cell death based on a cytotoxicity assay. Proteins were then harvested as noted earlier.

For the proteomic analyses, internal standard was added to all treated and untreated protein samples (1:1), and the protein mixture was subjected to disulfide reduction by incubation for 2.5 h at 37 °C in 1 mM dithiothreitol, followed by thiol alkylation by 5.5 mM iodoacetamide for 40 min at ambient temperature in the dark. Proteins were then digested with 50:1 (w/w) trypsin overnight at 37 °C. Peptide mixtures were loaded onto a Vydac C18 trap column (150 μm × 10 mm; 5 μm diameter, 300 Å pore-size particle; Grace, Deerfield, IL) at flow rate of 5 μL/min and eluted onto a Vydac C18 analytical column (75 μm × 150 mm, 5 μm diameter, 300 Å pore-size particle) at 200 nL/min with a gradient of 2–98% acetonitrile with

DOI: 10.1021/acs.chemrestox.5b00004
Chem. Res. Toxicol. 2015, 28, 978–988

0.1% formic acid over 180 min. Eluted peptides were analyzed by mass spectrometric analysis on a QSTAR-XL system (Applied Biosystems/MDS Sciex, Foster City, CA). Data were obtained from three biological replicates. Acquired MS/MS spectra were parsed by Spectrum Mill (Agilent Technologies, Foster City, CA) and searched against Saccharomyces Genome Database (SGD). SILAC peptide and protein quantitation was performed with differential expression quantitation, and SILAC protein ratios were determined as the average of all peptide ratios assigned to the protein. Differential protein expression was determined by Student's t test between samples.

A total of 2381 high-confidence proteins with a false-discovery rate of 0.5% were identified in control and MMS-treated samples.[22] To control for protein expression regulated by transcription, rather than by translational control mechanisms, the protein expression data were corrected using microarray data from our previous studies with the same yeast strain and MMS treatment conditions.[6,27,28] After removing genes that show the same expression change (up, down, or no change) for both mRNA and protein, we identified 222 upregulated and 438 downregulated genes whose expression is significantly regulated by translational machinery (Table S3).

Gene Ontology Annotation. Gene functional categorization and pathway analysis were performed with DAVID Bioinformatics Resources 2011.[29] The annotated proteins are clustered according to the biological process branch of the Gene Ontology (GO) annotation. The statistical significance of over- or under-representation of proteins in each GO category was assessed using a hypergeometric distribution, and the significance indicated by the p values for each GO category.[29]

RESULTS

Establishing Equivalent Stress Conditions for Oxidizing and Alkylating Agents. A quantitatively meaningful comparative analysis of stress responses requires that cells experience equivalent levels of stress. To this end, we chose cytotoxicity as a common end point, with doses producing 80% lethality for a 1 h exposure to the four oxidizing agents ($ONOO^-$, H_2O_2, γ-rad, TBHP) and five alkylating agents (MMS, EMS, IMS, MMNG, MNU), the structures of which are shown in Figure 2. The dose–response curves for the nine

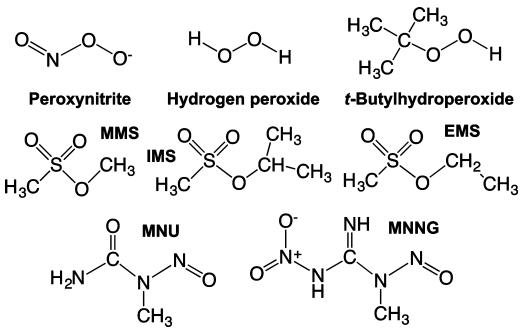

Figure 2. Structures of the oxidizing and alkylating agents used in the studies.

agents are shown in Figure S1, from which we determined LD_{80} doses of 5 mM H_2O_2, 25 mM TBHP, 0.8 mM $ONOO^-$, 510 G γ-radiation (116 Gy/min), 24 mM MMS, 190 mM EMS, 50 mM IMS, 82 mM MNNG, and 3 mM NMU. To assess the role of Trm140, which methylates C3 of cytosine at position 32 in several tRNAs (see below), in the cellular response to alkylating agent exposures, cell survival was determined for wild-type and Δ*trm140* mutant *S. cerevisiae* exposed to the alkylating agents at LD_{80} doses determined for wild-type cells. As shown in Figure S3, loss of Trm140 modestly but significantly increased the sensitivity of the cells to S_N2 alkylating agents MMS and EMS but not the other three S_N1 alkylating agents.

Quantifying Exposure-Induced Changes in the Full Set of tRNA Modifications. Having defined equivalent exposure conditions, the effect of exposure to nine different agents on the relative quantities of 23 tRNA modifications was determined using LC-MS/MS. The analysis consisted of five biological replicate sets of samples each comprised of three unexposed controls and one exposure for each of the nine agents. Normalized mass spectrometric (MS) signal intensities for each modification in the three unexposed controls were averaged, and changes in the MS signal intensities for the exposed samples were determined relative to this control value. Table S1 shows the complete set of 1380 data elements for the five biological replicates of this analysis, with the mean fold-change for each ribonucleoside and each exposure shown in Table S2. The results reveal that the levels of 22 of the 23 modified ribonucleosides were changed significantly by the various exposures ($p < 0.05$ by Student's t test); only m^5U did not change significantly (Table S2).

Stress Induces Reprogramming of tRNA Modifications with Unique Class- and Agent-Specific Patterns. To identify exposure-dependent patterns in the relative quantities of tRNA modifications in cells exposed to the nine toxicants, the fold-change data in Tables S1 and S2 were subjected to hierarchical clustering analysis, with the heat map representations shown in Figures 3 and S3. Analysis of the averaged data sets in Figure 3 shows clear class-specific distinctions for the groups of oxidizing agents and alkylating agents. All alkylating agents caused significant ($p < 0.05$) increases in Um, m^2G, mcm^5s^2U, mcm^5U, and m^1A, but these modifications were not significantly affected by the oxidizing agents. Furthermore, levels of yW and m^1I decreased significantly in all alkylator-exposed cells, but the changes in oxidant-exposed cells were not significant. In contrast, the levels of ncm^5U, m^5C, and i^6A did not change in cells exposed to any of the alkylating agents, but they increased significantly in response to all oxidizing agents. In addition to these class-specific signature patterns of modified ribonucleosides, there were also "sub-signatures" apparent for both classes of toxicant. This is most apparent for the alkylating agents, for which S_N2 alkylating agents[30] (EMS, MMS) cause increases in m^3C and m^7G, whereas S_N1 alkylating agents[30] (IMS, MNNG, MNU) uniquely increase Am (Figure 3).

A Data-Driven Model for Distinguishing Alkylation and Oxidation Stresses. The class- and agent-specific distinctions revealed by clustering analysis suggested that the stress-specific patterns of tRNA modifications could be used to predict exposure chemistry. To test this hypothesis, we developed a data-driven model (Figure 4A) using the K-nearest neighbor classification method to classify and predict the agent classes in term of tRNA modification spectra. Following 20 training and test cycles of supervised learning, a stable model (standard error <2%) was established. As shown in the confusion matrix in Figure 4B, which reports the average number of false positives, false negatives, true positives, and true negatives, the model proved to have sensitivities of 95% for the alkylating agent-exposed group (AA), 94% for oxidant exposures (OX), and 78% for unexposed cells (CT). The predictive specificities are 95% for AA, 76% for OX, and 98% for CT (Figure 4C). On the basis of this model, a set of 14 modified ribonucleosides was identified as contributing the most to distinguishing the exposures, with the group for

DOI: 10.1021/acs.chemrestox.5b00004
Chem. Res. Toxicol. 2015, 28, 978–988

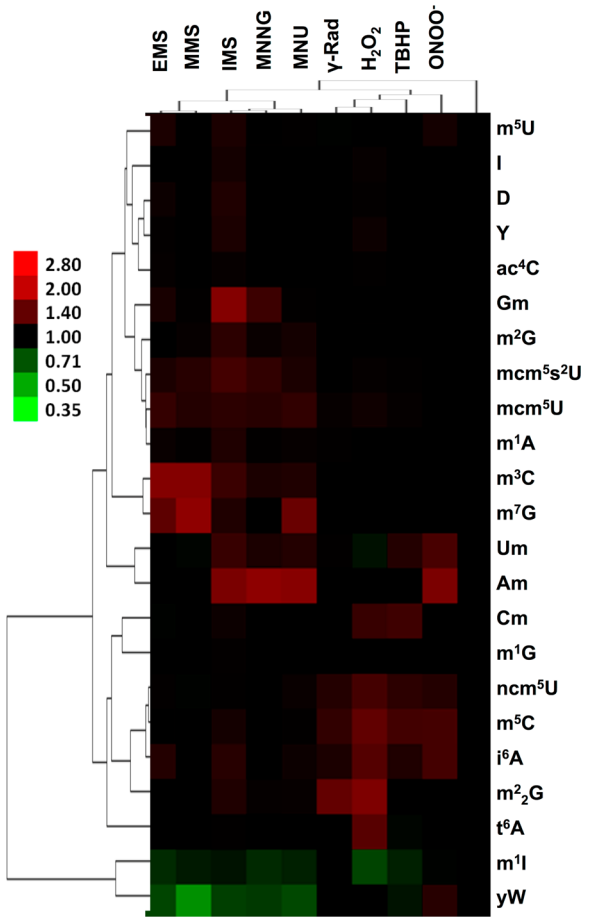

Figure 3. Hierarchical clustering analysis of average fold-change values for tRNA modifications in total tRNA from cells exposed to equitoxic (LD_{80}) doses of different alkylating agents and oxidizing agents. On the basis of the dose−response curves shown in Figure S1, budding yeast cells were exposed to LD_{80} doses of the various agents, and tRNA modifications were quantified by LC-MS/MS. The fold-change values (Table S2, with significance testing) were derived from the average of normalized MS signal intensity data from five biological replicates (Figure S2 and Table S1), and hierarchical clustering analysis was performed in log space (log_2).

predicting alkylating agents composed of m^3C, m^7G, yW, mcm^5U, Am, Gm, m^5C, mcm^5s^2U, and m^1I, and those for identifying oxidizing agent-exposures consisting of m^5C, m^3C, m^7G, Gm, ncm^5U, $m^2{}_2G$, i^6A, yW, and Cm (Table 1). These features match those revealed in the hierarchical clustering analysis (Figure 3).

Linking tRNA Modification Patterns to Selective Translation: Analysis of MMS-Induced Changes in the Proteome. The observation that S_N2 alkylating agents caused differential upregulation of m^3C in tRNA is reminiscent of H_2O_2-induced increases in m^5C (Figure 3) that led to selective translation of mRNAs enriched in the Leu codon TTG.[8] In addition, the increase in mcm^5U following MMS exposure has been linked to Trm9 and to the selective translation of mRNAs enriched with the Arg codon AGA.[6,19] Following this line of logic with MMS-treated cells, m^3C is present at position 32 of the anticodon loop of $tRNA^{Thr(IGU)}$, $tRNA^{Ser(UGA)}$, and $tRNA^{Ser(CGA)}$ in *S. cerevisiae*, with these tRNAs reading codons ACT, TCA and TCG, respectively.[31] Position 32 is adjacent to the anticodon (positions 34−36) and has the potential to modulate codon−anticodon interactions. It was thus hypothesized that MMS treatment would cause upregulation of proteins containing high levels of Thr and Ser. To test this hypothesis, we performed a comparative analysis of MMS-altered protein expression in *S. cerevisiae* using SILAC proteomics to quantify soluble proteins.[22] This analysis yielded 2381 high-confidence proteins with a false-discovery rate of 0.5%.[22] To control for protein expression regulated by transcription, rather than by translational control mechanisms, we corrected the protein expression data using microarray data from our previous studies with the same yeast strain and MMS treatment conditions.[6,27,28] After removing genes that show the same expression change (up, down, or no change) for both mRNA and protein, we identified 222 upregulated and 438 downregulated genes whose expression is significantly regulated by translational machinery (Table S3). This corrected index of protein expression was then evaluated for codon usage to test the hypothesis that MMS alters translational efficiency of genes with biased use of codons related to m^3C. To minimize the possibility that the influence of m^3C is counterbalanced by other functional constraints, we considered only proteins with high usage of optimal codons (each being >3% of the total codons in the gene for the protein). Among the Thr codons regulated by $tRNA^{Thr(IGU)}$ (Thr^{ACA}, Thr^{ACC}, Thr^{ACG}, Thr^{ACT}) and Ser codons regulated by $tRNA^{Ser(UGA)}$ and $tRNA^{Ser(CGA)}$ (Ser^{TCA}, Ser^{TCG}), only Thr^{ACC} and Thr^{ACT} are optimal codons, which are more efficiently translated and more frequently used by yeast genome in comparison with other synonymous codons (Thr^{ACA}, Thr^{ACG}).[32] As a result, other codons are rarely used, and their influence is therefore limited. Indeed, less than 20 of 660 MMS-altered proteins identified in this study have significantly high usage of these nonoptimal codons (hypergeometric distribution, $p < 0.01$; yeast genome as background). However, as shown in Figure 5A,B, genes upregulated by MMS treatment are significantly skewed to higher usage of Thr^{ACC} and Thr^{ACT} codons in comparison with downregulated genes (Student's *t* test; Thr^{ACC}, $p = 3.8 \times 10^{-09}$; Thr^{ACT}, $p = 8.0 \times 10^{-7}$). This is also apparent as a shift in the distribution of proteins with different ACC and ACT codon content (Figures 5C,D; Kolmogorov−Smirnov test: Thr^{ACC}, $p = 3.7 \times 10^{-06}$, Thr^{ACT}, 1.9×10^{-5}). The Thr^{ACC} codon is significantly enriched in 13% of upregulated genes (29 of 222; hypergeometric distribution, $p < 0.01$, with yeast genome as background), whereas only 7.5% of downregulated genes (33 of 438) have high usage of this codon (chi-squared test: $\chi^2 = 5.29$, $p = 0.021$) (Figure 5E). Similarly, the Thr^{ACT} codon is overrepresented in 9.0% of upregulated genes (20 of 222; hypergeometric distribution, $p < 0.01$) but only in 4.1% of downregulated genes (18 of 438) (chi-squared test: $\chi^2 = 6.52$, $p = 0.011$) (Figure 5F). Furthermore, if we consider the summed usage of the four Thr codons and two Ser codons from tRNAs possessing m^3C, then no significant difference is observed between up- and downregulated genes, indicating the overrepresentation of Thr^{ACC} and Thr^{ACT} codons in upregulated genes is not due to the overall high usage of Thr and Ser in the proteins. These results support the idea that the four Thr codons are differentially recognized by m^3C-modified $tRNA^{Thr}$ and that m^3C-modified $tRNA^{Thr}$ predominantly interacts with ACU and ACC to enhance translation. An analysis of statistically significant use of ACC and ACT codons in genes in Gene Ontology categories reveals highly significant enrichment of translation functions in genes upregulated by MMS and in intermediary metabolism categories in genes downregulated by MMS, as shown in Figure S4.

DOI: 10.1021/acs.chemrestox.5b00004
Chem. Res. Toxicol. 2015, 28, 978−988

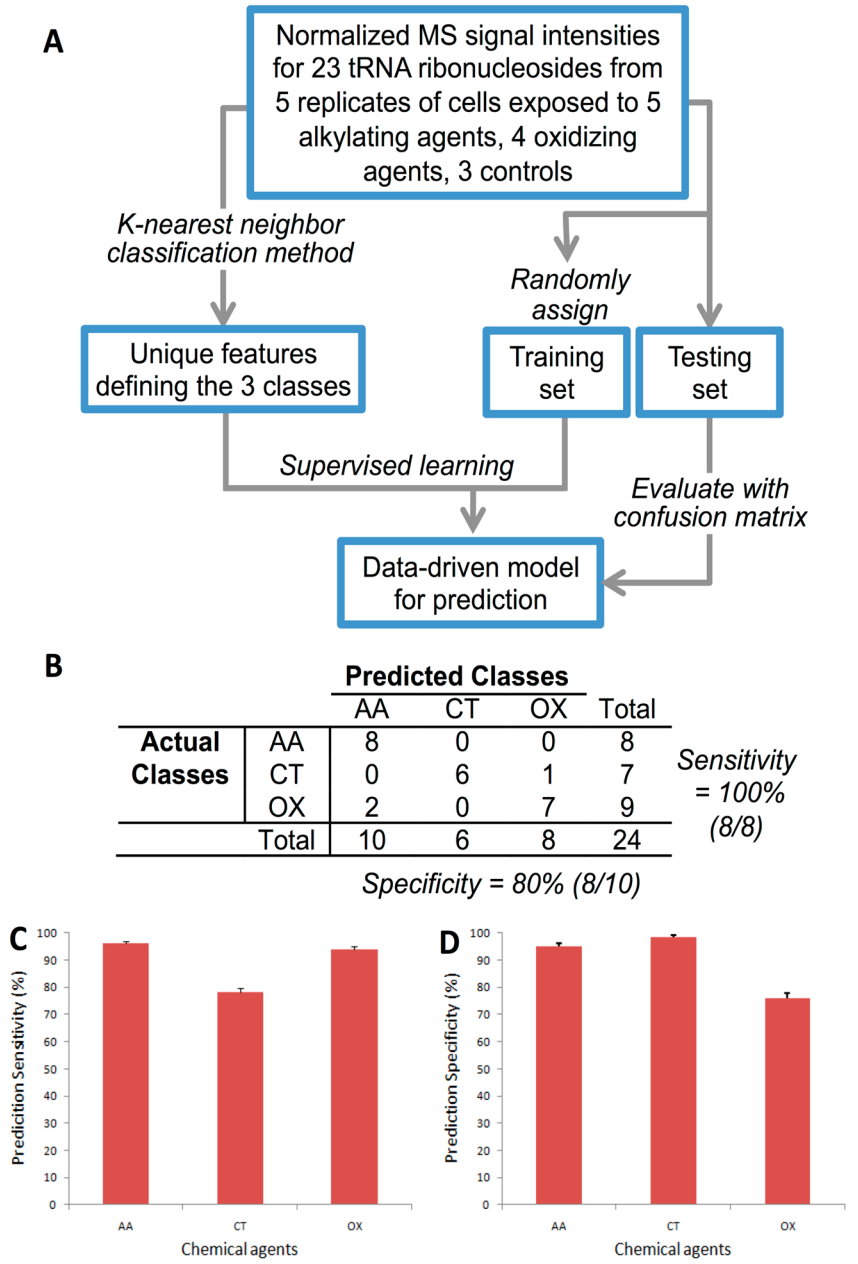

Figure 4. A data-driven model to define the ability of tRNA modification spectra to distinguish different stresses. K-nearest neighbor classification was used to develop a data-driven model (A) for the normalized MS signal intensities for each biological replicate of treated and control cells (Table S1; hierarchical clustering analysis of data sets shown in Figure S3). A confusion matrix (B) shows the number of false positives, false negatives, true positives, and true negatives that were used to determine prediction sensitivity (C) and prediction specificity (D) of the model, based on a total of 20 training and test cycles. A low standard error (<2%) demonstrates the stability of the data-driven model.

DISCUSSION

We recently discovered a system of translational control of the cellular stress response, in which stress-induced reprogramming of the two-dozen modified ribonucleosides in tRNA causes the selective translation of codon-biased mRNAs for critical response proteins.[6−8,33] The studies revealed that mechanistically different chemical stressors produced signature patterns of changes in the relative quantities of the various tRNA modifications. For example, H_2O_2 treatment increased the levels of Cm, m^5C and $m^2{}_2G$, whereas HOCl, $NaAsO_2$ and MMS either did not affect these modifications or lowered their levels.[7] These results raised the question of the predictive power of tRNA modification patterns to identify a specific stressor and to distinguish among chemically similar stressors. To address these questions, we developed a convergent platform of bioanalytical and mathematical tools to perform a systems-level analysis of patterns of change in the tRNA modifications in cells exposed to four oxidizing agents and five alkylating agents. This highly precise analysis (12% variance among biological replicates; see ref 7) revealed significant class-specific features that distinguished oxidizing agents from alkylating agents (Figure 3), with 14 modifications forming the basis for a data-driven model that predicted toxicant chemistry with >80% sensitivity and specificity (Figure 4). Furthermore, tRNA modification spectra distinguished S_N1 from S_N2 alkylating agents, with S_N2 agents causing a coordinated increase in m^3C and selective translation of

DOI: 10.1021/acs.chemrestox.5b00004
Chem. Res. Toxicol. 2015, 28, 978−988

Table 1. tRNA Modifications That Contribute Most Significantly to the Data-Driven Model for Predicting Exposure Chemistry[a]

rN[1]	tRNA	position	modifying enzyme	rN[1]	tRNA	position	modifying enzyme
Modifications Increased by Alkylating Agents				Modifications Increased by Oxidizing Agents			
m^3C	multiple	32, e2	Trm140	m^5C	$tRNA^{LeuCAA}$	34	Trm4
m^7G	multiple	46	Trm8, Trm82		$tRNA^{PheGAA}$	40	Trm4
mcm^5U	$tRNA^{ArgUCU}$	34	Trm9, Elp1-6, Kti11-13		multiple	48	Trm4
mcm^5s^2U	$tRNA^{GluUUC}$	34	Trm9, Nfs1, Elp1-6, KTI11-13		multiple	49	Trm4
Am	$tRNA^{HisGUG}$	4	unknown	ncm^5U	$tRNA^{ValUAC}$	34	Elp1-6, Kti11-13
Gm	multiple	18	Trm3	$m^2{}_2G$	multiple	26	Trm1
	$tRNA^{PheGAA}$	34	Trm7	i^6A	multiple	37	Mod5
m^2G	multiple	10	Trm11	*Cm*	multiple	32	Trm7
	$tRNA^{ValCAC}$	26	unknown		$tRNA^{TrpCCA}$	34	Trm7
Modifications Decreased by Alkylating Agents					multiple	4	unknown
yW	$tRNA^{PheGAA}$	37	Trm5				
m^1I	$tRNA^{AlaIGC}$	37	Tad1, Trm5				

[a]The modified ribonucleosides (rN) are organized into three groups, depending on whether their levels increased or decreased in response to the two classes of chemical stress (alkylating agents; oxidizing agents). Specific tRNAs are noted if the modification is located in a single tRNA species. Information was from Modomics Database,[10] Saccharomyces Genome Database,[43] and D'Silva et al.[57] The link between m^3C and cell response to S_N2 alkylating agents MMS and EMS is shown in Figure S3, in which it is shown that loss of Trm140 confers sensitivity these agents.

threonine-rich membrane proteins derived from ACT-rich genes. These results establish tRNA modifications as predictive biomarkers of exposure and illustrate a novel regulatory mechanism for translational control of cell stress response.

tRNA Modification Spectra as Biomarkers of Exposure. The class-specific patterns in the spectrum of tRNA modifications revealed by hierarchical clustering analysis (Figure 3) motivated the development of a data-driven model to assess the predictive power of the system of modified ribonucleosides. Such a model would provide insights into biological function of the system and the utility of tRNA modifications as biomarkers of exposure. The resulting model identified 14 of 25 tRNA modifications in *S. cerevisiae* as contributing most significantly to distinguishing the two classes of agents. As discussed shortly, several of these modified ribonucleosides have been observed to play roles in the cellular response to H_2O_2 and MMS exposures,[6−8] including m^5C, mcm^5U, and mcm^5s^2U, which supports the biological relevance of the model. The predictive power of the model, as revealed by confusion matrix analysis, was remarkably strong, with overall sensitivity and specificity over 80%. Examination of the individual specificity and sensitivity for oxidants and alkylating agents, however, revealed that the model had greater predictive power for the latter (>95% sensitivity and specificity versus 76−78% for oxidants; Figure 4). Although the basis for this difference is unclear, it is possible that alkylating agents produce a more complicated or extensive response in terms of activating more gene expression or requiring a broader set of responses than oxidizing agents for the same level of cytotoxicity. By any mechanism, it is striking that changes in the levels of 14 modified ribonucleosides are highly predictive of exposure chemistry in a manner similar to that with transcriptional profiling, proteomics, and metabolomics.[34−37] The predictive power of the tRNA modifications likely lies in their link to the system of biased codon use in families of stress response genes, for which we have observed that different stresses uniquely upregulate specific sets of survival and damage mitigation genes.[6−8,20,22,33] While further study is needed to compare the predictive power of tRNA modification patterns relative to other large 'omic data sets following exposure to these toxicants, the apparent mechanistic interdependence of tRNA modifications, selective translation of survival proteins, and the resulting changes in cell phenotype suggests the potential for strongly parallel and complementary biomarker signatures.

Assigning Biological Function to Stress-Predictive Ribonucleosides. While some of the stress-regulated modified ribonucleosides in Table 1 are located at more than one position in a tRNA and in multiple tRNA species, which complicates interpretation of their biological function, 10 of them are found in the anticodon loop, which suggests possible involvement in codon recognition and interactions with aminoacyl-tRNA synthetases.[38] A mechanistic link between stress-induced tRNA reprogramming and cell stress response is illustrated by oxidation-induced increases in the level of m^5C (Figure 3). Among other positions in several tRNAs, m^5C is located at the wobble position of $tRNA^{Leu(CAA)}$ that reads the UUG in mRNA, and it confers resistance to H_2O_2 by regulating translation of critical stress response proteins from TTG-enriched genes.[8] So, it is not surprising that m^5C appears in the basis set of 14 ribonucleosides in the model. Similar arguments can be made for other ribonucleosides in the basis set (Table 1), several of which are located in a single species of tRNA (mcm^5U, mcm^5s^2U, m^3C, Am, yW, m^1I). For example, alkylating agent-induced increases in the relative levels of mcm^5U and mcm^5s^2U (Figure 3), which are part of the 14 ribonucleoside basis set for the exposure model, are consistent with our observation that modification of the wobble position of $tRNA^{Arg(UCU)}$ with mcm^5U confers resistance to MMS by promoting the translation of proteins from genes enriched with the cognate AGA codon, which represent a specific group of DNA damage-response genes.[6] So, again, it is not surprising to see elevations of mcm^5U and mcm^5s^2U in MMS-exposed cells. While changes in the number of copies of specific tRNAs could contribute to the stress-induced changes in levels of tRNA modifications, along with increased modifying enzyme activity, our previous tRNA-seq analysis revealed that H_2O_2 and MMS induced nearly identical patterns of up- and downregulation for 58 tRNAs, with 18 tRNAs showing opposing changes for the stresses.[39]

Analogous arguments may provide insights into the role of other stress-regulated ribonucleosides in Table 1. For example, yW and m^1I are Trm5-dependent modifications that are downregulated by exposure to the alkylating agents (Figure 3), with yW located at position 37 of $tRNA^{Phe(GAA)}$ and m^1I located

DOI: 10.1021/acs.chemrestox.5b00004
Chem. Res. Toxicol. 2015, 28, 978−988

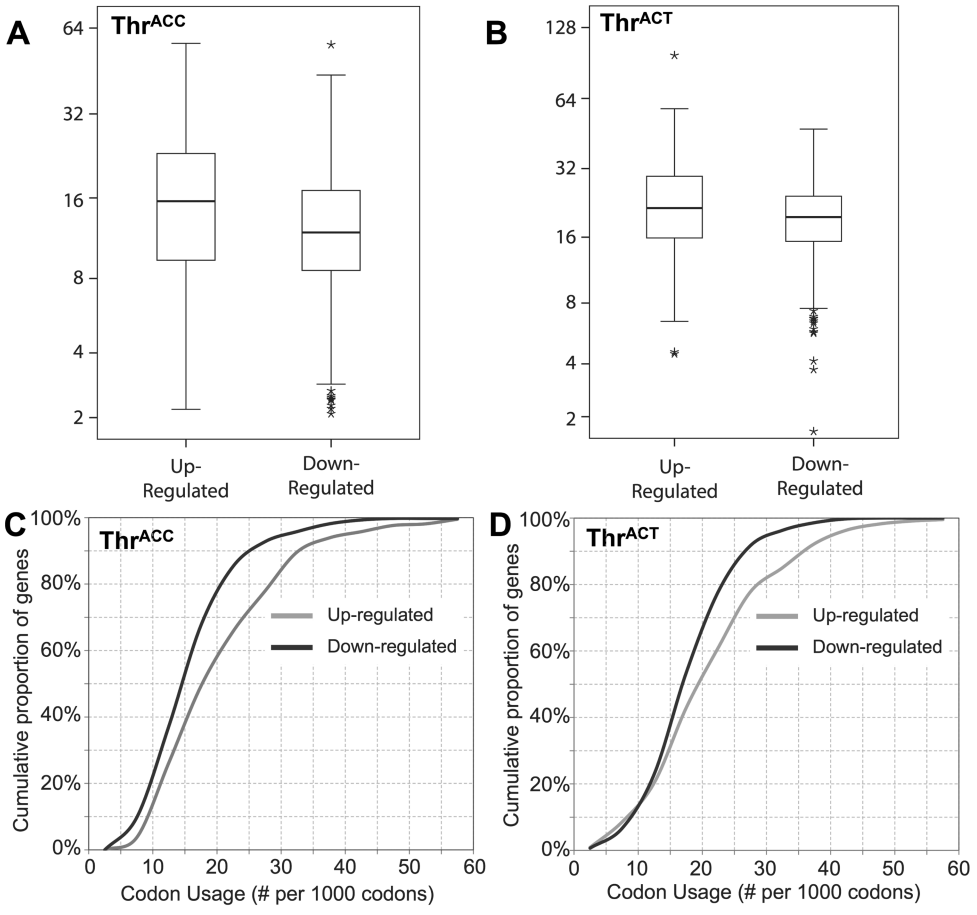

E

ThrACC	Up-regulated	Down-regulated
Enriched	29	33
Non-enriched	193	405
Total	222	438
	p-value = 0.021	

F

ThrACT	Up-regulated	Down-regulated
Enriched	20	18
Non-enriched	202	420
Total	222	438
	p-value = 0.011	

Figure 5. Proteomic analysis reveals that exposure to the S_N2 alkylating agent, MMS, causes selective translation of mRNAs possessing biased use of the threonine codons ACC and ACT that are decoded by of $tRNA^{Thr(IGU)}$, one of three tRNAs possessing MMS-regulated m^3C at position 34 (Figure 3). SILAC-based proteomic analysis revealed that MMS treatment induced up- or downregulation of 694 of 2381 proteins independent of changes in mRNA levels (Table S3). The upper box plots show that the threonine codons ACC (A) and ACT (B) are used significantly more frequently in genes for proteins upregulated by MMS exposure than in downregulated proteins, with significance demonstrated by a Student's *t* test ($p = 3.8 \times 10^{-9}$ and $p = 8.0 \times 10^{-7}$, respectively). Similarly, the distribution plots in middle panels C and D demonstrate a significant MMS-induced shift in the population of proteins enriched in codons ACC (C) and ACT (D), with significance demonstrated by a Kolmogorov–Smirnov test ($p = 3.7 \times 10^{-6}$ and 1.9×10^{-5}, respectively). The lower tables show that the threonine codons ACC (E) and ACT (F) are significantly enriched in genes upregulated by MMS exposure (29 of 222; hypergeometric distribution, $p < 0.01$), whereas the codons are under-represented relative to genome averages in genes downregulated by MMS (chi-squared test: ACC, $\chi^2 = 5.29$, $p = 0.021$; ACT, $\chi^2 = 6.52$, $p = 0.011$). Figure S4 shows an analysis of statistically significant use of ACC and ACT codons in MMS-regulated genes (Table S3) in Gene Ontology categories, and Table S4 lists proteins with threonine content >10%.

at the wobble position 34 of $tRNA^{Ala(IGC)}$, respectively. Niu and co-workers have shown that *trm5* is an essential gene involved in cell cycle regulation,[40] which raises the possibility that yW and m^1I play a role in regulating the translation of cell cycle proteins during the alkylation stress response. Further evidence for mechanistic linkage between stress-regulated tRNA modifications and the stress response arises in the observation of subclass signatures for both oxidizing (Am changes with $ONOO^-$ exposure) and alkylating agents (m^3C changes with S_N2 alkyllators MMS and EMS), as discussed next.

tRNA Modification Patterns Distinguish Different Oxidizing Agents. While the behavior is more striking for the alkylating agents, the four oxidizing agents each showed unique patterns of change in the 23 tRNA modifications (Figure 3 and Table S2). For example, $ONOO^-$ uniquely and significantly caused an increase in Am, whereas no significant change in this ribonucleoside was observed with the other three oxidizing agent samples (Table S2). The basis for this behavior may lie in the different chemistries of reactive oxygen species (ROS) and reactive nitrogen species (RNS) in terms of molecular damage.[41,42] Am is found only at position 4 of $tRNA^{His(GUG)}$ in *S. cerevisiae*.[10,43] Analysis of the yeast genome using the Codon Counting Database[44] reveals that the cognate codon for this tRNA, CAC, is found to be significantly enriched

DOI: 10.1021/acs.chemrestox.5b00004
Chem. Res. Toxicol. 2015, 28, 978–988

in 410 genes in the yeast genome (hypergeometric distribution, p value < 0.01; Table S4). Of these CAC-enriched genes, yeast flavohemoglobin is a nitric oxide oxidoreductase, which directly interacts with $ONOO^-$ and is involved in NO detoxification. It is well-known to play a role in the oxidative and nitrosative stress responses.[45]

Interestingly, among spectra of the other three oxidizing agents, H_2O_2 exposure is more similar to γ-rad than to another peroxide, TBHP. This may be due to the fact that H_2O_2 and γ-rad generate hydroxyl radicals that lead to chemically distinct types of molecular damage than the peroxyl radicals arising from TBHP. Thus, there is likely to be a discrete biological mechanism underlying the tRNA modification patterns for different chemical stresses, with the subclass signatures for S_N1 and S_N2 alkylating agents providing a striking illustration of the phenomenon.

Correlations between Subclass Signatures and Mechanisms of Action among Alkylating Agents. The hierarchical clustering analysis in Figure 3 reveals a significant differential alteration of modified ribonucleosides by the two chemically distinct types of alkylating agents. MMS and EMS represent one class of alkylating agent that appears to react with nucleophilic sites in nucleic acids, proteins, and other cellular molecules[46,47] by a bimolecular nucleophilic substitution reaction (S_N2), whereas IMS, MNNG and NMU appear to react by a unimolecular mechanism (S_N1).[48] The relevance of this mechanistic classification for genetic toxicology has been challenged[49] but the two groups of alkylating agents produce distinctly different types of molecular damage,[48] and we use the S_N1/S_N2 nomenclature for the sake of clarity. The analyses in Figure 3 and Table S2 clearly and significantly distinguish MMS and EMS from the other three agents in terms of tRNA modification spectra. For example, the relative levels of m^7G and m^3C in MMS- and EMS-exposed cells increased more significantly than in IMS-, MNNG-, and NMU-exposed cells. In contrast, the levels of Am and Um did not change in response to MMS and EMS, but they were elevated when cells were treated with the other three alkylating agents. These results suggest that the cells are responding to the damage caused by two classes of alkylating agents with different translational responses that reflect activation of different cellular survival pathways. This point was demonstrated in 1983 by Smith and Grisham[50] in studies of cytotoxicity in yeast. They observed that the toxicity of S_N2 alkylating agents, such as MMS, arises mainly by damage to membrane proteins, whereas the toxicity of S_N1 alkylating agents, such as MNNG, results from interference with DNA replication.[50] Our data provide a mechanistic model for these observations. The S_N2 agents, MMS and EMS, increased the level of m^3C, which is known to occur at position 32 of $tRNA^{Thr(IGU)}$, $tRNA^{Ser(UGA)}$, and $tRNA^{Ser(CGA)}$ and in the variable stem of a Ser tRNA.[51−53] The link between these tRNAs and the proposed membrane protein target of S_N2 agents may lie in the fact that Thr and Ser are significantly enriched in membrane proteins in eukaryotes.[54−56] Analysis of the *S. cerevisiae* genome reveals that, on average, 5.9% of each yeast protein is composed of Thr, whereas only 83 of ∼6000 genes in the yeast genome code for proteins composed of >10% Thr[29] (Tables S4 and S5). Functional analysis of the Thr-enriched proteins by annotation with Gene Ontology functional attributes using the DAVID bioinformatics resources[29] revealed that 61 of these 83 genes code for cell wall and cell membrane proteins (Tables S5 and S6). While membrane proteins were not well represented in our proteomic analysis, which is to be expected given the predominance of soluble proteins in our isolation method, there was a significant upregulation of proteins from genes enriched with Thr^{ACT} and the optimal codon Thr^{ACC} in cells exposed to MMS (Figure 5). Along with the observation that loss of the ability synthesize m^3C confers sensitivity to EMS and MMS in Δ*trm140* cells (Figure S2), these results are consistent with the idea that the EMS- and MMS-induced increase in m^3C reflects the need for more efficient translation of Thr-enriched membrane proteins in the response of *S. cerevisiae* to exposure to the S_N2 alkylating agents. There are certainly factors other than reprogramming of m^3C-cointaining tRNAs and selective translation of ACT- and ACC-enriched genes in the translational control of the MMS stress response, as suggested by the downregulation of some proteins from ACT- and ACC-enriched genes (Figure 5), such as contributions from tRNA modifications and biased codon usage, as well as factors regulating tRNA charging, ribosome loading, and translational elongation rates.

CONCLUSIONS

We employed novel bioanalytical and computational tools to demonstrate that cells respond to exposure to different classes of chemical stressors by reprogramming a system of modified ribonucleosides in tRNA, with unique patterns distinguishing the class of chemicals, as well as the subclass. Multivariate statistical analysis and data-driven modeling of the tRNA modification patterns proved to be highly predictive of toxicant chemistry, with bioinformatic and proteomic analyses establishing a mechanistic link among exposure, tRNA modifications, and codon-biased translation of response proteins. With implications for other organisms, including humans, these results establish tRNA modifications as predictive biomarkers of exposure and illustrate a novel regulatory mechanism for translational control of cell stress response.

ASSOCIATED CONTENT

Supporting Information

Cytotoxicity dose−response curves; hierarchical clustering analysis of stress-induced changes in tRNA modification levels; sensitivity of Trm140 to the five alkylating agents; analysis of MMS effects on expression of genes with significant use of ACC and ACT codons in genes in Gene Ontology categories; toxicant-induced changes in tRNA modifications; average fold-change values for toxicant-induced changes in tRNA modifications; MMS-induced up- or downregulation of 694 of 2381 proteins that is independent of changes in mRNA levels; and proteins with threonine content >10% are membrane- and cell wall-related proteins. This material is available free of charge via the Internet at http://pubs.acs.org.

AUTHOR INFORMATION

Corresponding Author

*Tel.: 617-253-8017; E-mail: pcdedon@mit.edu.

Present Addresses

[⊥](C.T.Y.C.) Institute for Medical Engineering and Science, Massachusetts Institute of Technology, Cambridge, Massachusetts 02139, United States.

[#](W.D.) Clinical Proteomics Research Center, Department of Neurology, Massachusetts General Hospital, Boston, Massachusetts 02114, United States.

DOI: 10.1021/acs.chemrestox.5b00004
Chem. Res. Toxicol. 2015, 28, 978−988

○(F.L.) Dana-Farber Cancer Institute, Boston, Massachusetts 02215, United States.

Author Contributions

▽C.T.Y.C. and W.D. contributed equally to this work.

Funding

This work was supported by grants from the National Science Foundation (CHE-1308839), the U.S. National Institute of Environmental Health Science (ES002109, ES017010) and National Cancer Institute (CA026731), and the Singapore−MIT Alliance for Research and Technology sponsored by the National Research Foundation of Singapore.

Notes

The authors declare no competing financial interest.

■ ACKNOWLEDGMENTS

The authors gratefully acknowledge the MIT Center for Environmental Health Sciences for use of the Bioanalytical Facilities Core for quantifying modified ribonucleosides and performing proteomic analyses.

■ ABBREVIATIONS

EMS, ethyl methanesulfonate; IMS, isopropyl methanesulfonate; LC-MS/MS, liquid chromatography-coupled tandem quadrupole mass spectrometry; MMS, methyl methanesulfonate; MNNG, *N*-methyl-*N*′-nitro-*N*-nitrosoguanidine; MS, mass spectrometry; NMU, *N*-nitro-*N*-methylurea; $ONOO^-$, peroxynitrite; TBHP, *t*-butyl hydroperoxide; γ-rad, γ-radiation

■ REFERENCES

(1) Currie, R. A. (2012) Toxicogenomics: the challenges and opportunities to identify biomarkers, signatures and thresholds to support mode-of-action. *Mutat. Res. 746*, 97−103.

(2) Slikker, W., Jr., Paule, M. G., Wright, L. K., Patterson, T. A., and Wang, C. (2007) Systems biology approaches for toxicology. *J. Appl. Toxicol. 27*, 201−217.

(3) Jacobs, A. T., and Marnett, L. J. (2010) Systems analysis of protein modification and cellular responses induced by electrophile stress. *Acc. Chem. Res. 43*, 673−683.

(4) Rusyn, I., Fry, R. C., Begley, T. J., Klapacz, J., Svensson, J. P., Ambrose, M., and Samson, L. D. (2007) Transcriptional networks in *S. cerevisiae* linked to an accumulation of base excision repair intermediates. *PLoS One 2*, e1252.

(5) Rooney, J. P., George, A. D., Patil, A., Begley, U., Bessette, E., Zappala, M. R., Huang, X., Conklin, D. S., Cunningham, R. P., and Begley, T. J. (2009) Systems based mapping demonstrates that recovery from alkylation damage requires DNA repair, RNA processing, and translation associated networks. *Genomics 93*, 42−51.

(6) Begley, U., Dyavaiah, M., Patil, A., Rooney, J. P., DiRenzo, D., Young, C. M., Conklin, D. S., Zitomer, R. S., and Begley, T. J. (2007) Trm9-catalyzed tRNA modifications link translation to the DNA damage response. *Mol. Cell 28*, 860−870.

(7) Chan, C. T., Dyavaiah, M., DeMott, M. S., Taghizadeh, K., Dedon, P. C., and Begley, T. J. (2010) A quantitative systems approach reveals dynamic control of tRNA modifications during cellular stress. *PLoS Genet. 6*, e1001247.

(8) Chan, C. T., Pang, Y. L., Deng, W., Babu, I. R., Dyavaiah, M., Begley, T. J., and Dedon, P. C. (2012) Reprogramming of tRNA modifications controls the oxidative stress response by codon-biased translation of proteins. *Nat. Commun. 3*, 937.

(9) Rozenski, J., Crain, P. F., and McCloskey, J. A. (1999) The RNA Modification Database: 1999 update. *Nucleic Acids Res. 1*, 196−197.

(10) Czerwoniec, A., Dunin-Horkawicz, S., Purta, E., Kaminska, K. H., Kasprzak, J. M., Bujnicki, J. M., Grosjean, H., and Rother, K. (2009) Modomics: A database of RNA modification pathways. 2008 update. *Nucleic Acids Res. 37*, D118−D121.

(11) Agris, P. F., Vendeix, F. A., and Graham, W. D. (2007) tRNA's wobble decoding of the genome: 40 years of modification. *J. Mol. Biol. 366*, 1−13.

(12) Urbonavicius, J., Qian, Q., Durand, J. M., Hagervall, T. G., and Bjork, G. R. (2001) Improvement of reading frame maintenance is a common function for several tRNA modifications. *EMBO J. 20*, 4863−4873.

(13) Motorin, Y., and Helm, M. (2010) tRNA stabilization by modified nucleotides. *Biochemistry 49*, 4934−4944.

(14) Alexandrov, A., Chernyakov, I., Gu, W., Hiley, S. L., Hughes, T. R., Grayhack, E. J., and Phizicky, E. M. (2006) Rapid tRNA decay can result from lack of nonessential modifications. *Mol. Cell 21*, 87−96.

(15) Thompson, D. M., and Parker, R. (2009) Stressing out over tRNA cleavage. *Cell 138*, 215−219.

(16) Netzer, N., Goodenbour, J. M., David, A., Dittmar, K. A., Jones, R. B., Schneider, J. R., Boone, D., Eves, E. M., Rosner, M. R., Gibbs, J. S., Embry, A., Dolan, B., Das, S., Hickman, H. D., Berglund, P., Bennink, J. R., Yewdell, J. W., and Pan, T. (2009) Innate immune and chemically triggered oxidative stress modifies translational fidelity. *Nature 462*, 522−526.

(17) Emilsson, V., Naslund, A. K., and Kurland, C. G. (1992) Thiolation of transfer RNA in *Escherichia coli* varies with growth rate. *Nucleic Acids Res. 20*, 4499−4505.

(18) Begley, U., Sosa, M. S., Avivar-Valderas, A., Patil, A., Endres, L., Estrada, Y., Chan, C. T., Su, D., Dedon, P. C., Aguirre-Ghiso, J. A., and Begley, T. (2013) A human tRNA methyltransferase 9-like protein prevents tumour growth by regulating lin9 and hif1-alpha. *EMBO Mol. Med. 5*, 366−383.

(19) Patil, A., Chan, C. T., Dyavaiah, M., Rooney, J. P., Dedon, P. C., and Begley, T. J. (2012) Translational infidelity-induced protein stress results from a deficiency in trm9-catalyzed tRNA modifications. *RNA Biol. 9*, 990−1001.

(20) Patil, A., Dyavaiah, M., Joseph, F., Rooney, J. P., Chan, C. T., Dedon, P. C., and Begley, T. J. (2012) Increased tRNA modification and gene-specific codon usage regulate cell cycle progression during the DNA damage response. *Cell Cycle 11*, 3656−3665.

(21) Dudley, E., Tuytten, R., Bond, A., Lemiere, F., Brenton, A. G., Esmans, E. L., and Newton, R. P. (2005) Study of the mass spectrometric fragmentation of pseudouridine: comparison of fragmentation data obtained by matrix-assisted laser desorption/ionisation post-source decay, electrospray ion trap multistage mass spectrometry, and by a method utilising electrospray quadrupole time-of-flight tandem mass spectrometry and in-source fragmentation. *Rapid Commun. Mass Spectrom. 19*, 3075−3085.

(22) Deng, W., Begley, T. J., and Dedon, P. C. (2015) Trm9-catalyzed tRNA modifications promote translation by directly regulating expression of ribosomal proteins, submitted for publication..

(23) de Godoy, L. M., Olsen, J. V., Cox, J., Nielsen, M. L., Hubner, N. C., Frohlich, F., Walther, T. C., and Mann, M. (2008) Comprehensive mass-spectrometry-based proteome quantification of haploid versus diploid yeast. *Nature 455*, 1251−1254.

(24) Gruhler, A., Olsen, J. V., Mohammed, S., Mortensen, P., Faergeman, N. J., Mann, M., and Jensen, O. N. (2005) Quantitative phosphoproteomics applied to the yeast pheromone signaling pathway. *Mol. Cell. Proteomics 4*, 310−327.

(25) Bradford, M. M. (1976) A rapid and sensitive method for the quantitation of microgram quantities of protein utilizing the principle of protein-dye binding. *Anal. Biochem. 72*, 248−254.

(26) Ishihama, Y., Sato, T., Tabata, T., Miyamoto, N., Sagane, K., Nagasu, T., and Oda, Y. (2005) Quantitative mouse brain proteomics using culture-derived isotope tags as internal standards. *Nat. Biotechnol. 23*, 617−621.

(27) Begley, T. J., and Samson, L. D. (2004) Network responses to DNA damaging agents. *DNA Repair 3*, 1123−1132.

(28) Jelinsky, S. A., Estep, P., Church, G. M., and Samson, L. D. (2000) Regulatory networks revealed by transcriptional profiling of damaged saccharomyces cerevisiae cells: Rpn4 links base excision repair with proteasomes. *Mol. Cell. Biol. 20*, 8157−8167.

DOI: 10.1021/acs.chemrestox.5b00004
Chem. Res. Toxicol. 2015, 28, 978−988

(29) Huang, D. W., Sherman, B. T., and Lempicki, R. A. (2009) Systematic and integrative analysis of large gene lists using DAVID bioinformatics resources. *Nat. Protoc. 4*, 44−57.
(30) Chen, B. J., Carroll, P., and Samson, L. (1994) The *Escherichia coli* AlkB protein protects human cells against alkylation-induced toxicity. *J. Bacteriol. 176*, 6255−6261.
(31) Dunin-Horkawicz, S., Czerwoniec, A., Gajda, M. J., Feder, M., Grosjean, H., and Bujnicki, J. M. (2006) Modomics: a database of RNA modification pathways. *Nucleic Acids Res. 34*, D145−D149.
(32) Kliman, R. M., Irving, N., and Santiago, M. (2003) Selection conflicts, gene expression, and codon usage trends in yeast. *J. Mol. Evol. 57*, 98−109.
(33) Dedon, P. C., and Begley, T. J. (2014) A system of RNA modifications and biased codon use controls cellular stress response at the level of translation. *Chem. Res. Toxicol. 27*, 330−337.
(34) Auffray, C., Chen, Z., and Hood, L. (2009) Systems medicine: the future of medical genomics and healthcare. *Genome Med. 1*, 2.
(35) Merrick, B. A., and Bruno, M. E. (2004) Genomic and proteomic profiling for biomarkers and signature profiles of toxicity. *Curr. Opin. Mol. Ther. 6*, 600−607.
(36) Poste, G. (2011) Bring on the biomarkers. *Nature 469*, 156−157.
(37) van Doorn, M., Vogels, J., Tas, A., van Hoogdalem, E. J., Burggraaf, J., Cohen, A., and van der Greef, J. (2007) Evaluation of metabolite profiles as biomarkers for the pharmacological effects of thiazolidinediones in type 2 diabetes mellitus patients and healthy volunteers. *Br. J. Clin. Pharmacol. 63*, 562−574.
(38) Bjork, G. R. (1995) Biosynthesis and function of modified nucleosides, in *tRNA: Structure, biosynthesis and function* (Söll, D., and RajBhandary, U. L., Eds.) pp 165−205, ASM Press, Washington, DC.
(39) Pang, Y. L., Abo, R., Levine, S. S., and Dedon, P. C. (2014) Diverse cell stresses induce unique patterns of tRNA up- and down-regulation: tRNA-seq for quantifying changes in tRNA copy number. *Nucleic Acids Res. 42*, e170.
(40) Niu, W., Li, Z., Zhan, W., Iyer, V. R., and Marcotte, E. M. (2008) Mechanisms of cell cycle control revealed by a systematic and quantitative overexpression screen in *S. cerevisiae*. *PLoS Genet. 4*, e1000120.
(41) Dedon, P. C., and Tannenbaum, S. R. (2004) Reactive nitrogen species in the chemical biology of inflammation. *Arch. Biochem. Biophys. 423*, 12−22.
(42) Dizdaroglu, M. (1992) Oxidative damage to DNA in mammalian chromatin. *Mutat. Res. 275*, 331−342.
(43) Dwight, S. S., Balakrishnan, R., Christie, K. R., Costanzo, M. C., Dolinski, K., Engel, S. R., Feierbach, B., Fisk, D. G., Hirschman, J., Hong, E. L., Issel-Tarver, L., Nash, R. S., Sethuraman, A., Starr, B., Theesfeld, C. L., Andrada, R., Binkley, G., Dong, Q., Lane, C., Schroeder, M., Weng, S., Botstein, D., and Cherry, J. M. (2004) Saccharomyces genome database: underlying principles and organisation. *Briefings Bioinf. 5*, 9−22.
(44) Tumu, S., Patil, A., Towns, W., Dyavaiah, M., and Begley, T. J. (2012) The gene-specific codon counting database: A genome-based catalog of one-, two-, three-, four- and five-codon combinations present in *Saccharomyces cerevisiae* genes. *Database*, bas002.
(45) Cassanova, N., O'Brien, K. M., Stahl, B. T., McClure, T., and Poyton, R. O. (2005) Yeast flavohemoglobin, a nitric oxide oxidoreductase, is located in both the cytosol and the mitochondrial matrix: Effects of respiration, anoxia, and the mitochondrial genome on its intracellular level and distribution. *J. Biol. Chem. 280*, 7645−7653.
(46) Osterman-Golkar, S., and Bergmark, E. (1988) Alkylation of haemoglobin, plasma proteins and DNA in the mouse by diethylnitrosamine. *Carcinogenesis 9*, 1915−1917.
(47) Segerback, D., Calleman, C. J., Ehrenberg, L., Lofroth, G., and Osterman-Golkar, S. (1978) Evaluation of genetic risks of alkylating agents IV. Quantitative determination of alkylated amino acids in haemoglobin as a measure of the dose after-treatment of mice with methyl methanesulfonate. *Mutat. Res. 49*, 71−82.
(48) Singer, B. (1975) The chemical effects of nucleic acid alkylation and their relation to mutagenesis and carcinogenesis. *Prog. Nucleic Acid Res. Mol. Biol. 15*, 219−284.
(49) Loechler, E. L. (1994) A violation of the Swain−Scott principle, and not S_N1 versus S_N2 reaction mechanisms, explains why carcinogenic alkylating agents can form different proportions of adducts at oxygen versus nitrogen in DNA. *Chem. Res. Toxicol. 7*, 277−280.
(50) Smith, G. J., and Grisham, J. W. (1983) Cytotoxicity of monofunctional alkylating agents. Methyl methanesulfonate and methyl-*N*′-nitro-*N*-nitrosoguanidine have different mechanisms of toxicity for 10t1/2 cells. *Mutat. Res. 111*, 405−417.
(51) Weissenbach, J., Kiraly, I., and Dirheimer, G. (1977) Primary structure of tRNA Thr 1a and b from brewer's yeast. *Biochimie 59*, 381−391.
(52) Machnicka, M. A., Milanowska, K., Osman Oglou, O., Purta, E., Kurkowska, M., Olchowik, A., Januszewski, W., Kalinowski, S., Dunin-Horkawicz, S., Rother, K. M., Helm, M., Bujnicki, J. M., and Grosjean, H. (2013) Modomics: a database of RNA modification pathways—2013 update. *Nucleic Acids Res. 41*, D262−D267.
(53) Noma, A., Yi, S., Katoh, T., Takai, Y., Suzuki, T., and Suzuki, T. (2011) Actin-binding protein abp140 is a methyltransferase for 3-methylcytidine at position 32 of trnas in *Saccharomyces cerevisiae*. *RNA 17*, 1111−1119.
(54) Kitazoe, Y., Kishino, H., Hasegawa, M., Nakajima, N., Thorne, J. L., and Tanaka, M. (2008) Adaptive threonine increase in transmembrane regions of mitochondrial proteins in higher primates. *PLoS One 3*, e3343.
(55) Eilers, M., Shekar, S. C., Shieh, T., Smith, S. O., and Fleming, P. J. (2000) Internal packing of helical membrane proteins. *Proc. Natl. Acad. Sci. U.S.A. 97*, 5796−5801.
(56) Dawson, J. P., Weinger, J. S., and Engelman, D. M. (2002) Motifs of serine and threonine can drive association of transmembrane helices. *J. Mol. Biol. 316*, 799−805.
(57) D'Silva, S., Haider, S. J., and Phizicky, E. M. (2011) A domain of the actin binding protein abp140 is the yeast methyltransferase responsible for 3-methylcytidine modification in the tRNA anti-codon loop. *RNA 17*, 1100−1110.

DOI: 10.1021/acs.chemrestox.5b00004
Chem. Res. Toxicol. 2015, 28, 978−988